Fan Wu ORCID iD: 0000-0001-8621-9449

19-00427

Environmental Toxicology

Wu et al.

Running head: Environmentally friendly nano-*BuSn* for semiconductor

Monoalkyl Tin Nano-cluster Films Reveal a Low Environmental Impact Under Simulated Natural Conditions

Fan Wu,[a,e] Bryan J. Harper,[c] David A. Marsh,[d] Sumit Saha,[b] Trey Diulus,[a] Jenn M. Amador,[b] Douglas A. Keszler,[b] Gregory S. Herman,[a] Bettye L.S. Maddux,[a,b] Stacey L. Harper[a,c,*]

[a] School of Chemical, Biological and Environmental Engineering, Oregon State University, Corvallis, Oregon 97331 USA

[b] Department of Chemistry, Oregon State University, Corvallis, Oregon 97331 USA

[c] Department of Environmental and Molecular Toxicology, Oregon State University, Corvallis, Oregon 97331 USA

[d] Department of Chemistry, Alfred University, Alfred, New York 14802 USA

[e] School of Environment and Guangdong Key Laboratory of Environmental Pollution and Health, Jinan University, Guangzhou 510632, China

This article has been accepted for publication and undergone full peer review but has not been through the copyediting, typesetting, pagination and proofreading process, which may lead to differences between this version and the Version of Record. Please cite this article as doi: 10.1002/etc.4580.

(Submitted 25 June 2019; Returned for Revision 10 July 2019; Accepted 19 August 2019)

Abstract: Recently, monoalkyl oxo-hydroxo tin clusters have emerged as a new class of metal-oxide resist to support the semiconductor industry transition to extreme ultraviolet lithography (EUV). Under EUV exposure, these tin-based clusters exhibit higher performance and wider process windows than conventional polymer materials. A promising new monoalkyl precursor, $[(BuSn)_{12}O_{14}(OH)_6][OH]_2$ (BuSn), is still in its infancy in terms of film formation. However, understanding potential environmental effects could significantly affect future development as a commercial product. Here, we synthesize and explore the toxicity of these nano-BuSn in algae *Chlamydomonas reinhardtii* and crustaceans *Daphnia magna* at exposure concentrations ranging from 0 to 250 mg/L. The nano-BuSn had no effect on *C. reinhardtii* growth rate irrespective of concentration; whereas, high nanoparticle concentrations (≥100 mg/L) increased *D. magna* immobilization and mortality significantly. To simulate an end-of-life disposal and leachate contamination, *BuSn* coated film wafers were incubated in water at various pH, temperature for 14 and 90 days to investigate leaching rates and subsequent toxicity of the leachates. While small quantities of tin (1.1 – 3.4% of deposited mass) leached from the wafers, it was insufficient to elicit a toxic response regardless of pH, incubation time, or temperature. The low toxicity of the tin-based thin films suggests that they can be an environmentally friendly addition to the materials sets useful for semiconductor manufacturing.

Keywords: AFM; Ecotoxicity; Semiconductor; Organotin thin film; TOF-SIMS

This article includes online-only Supplemental Data.

(*) Corresponding Author: Stacey Harper – stacey.harper@oregonstate.edu

Published online XXXX 2019 in Wiley Online Library
(www.wileyonlinelibrary.com).
DOI: 10.1002/etc.xxxx

INTRODUCTION

Organotin compounds have found widespread industrial, commercial, and agricultural uses since the 1980s (Horiguchi 2017), with approximately 30,000 tons of organotin generated annually (Davies and Smith 1980). Trialkyltins are well-known for their powerful toxic action on the central nervous system, and they have been described as *"perhaps the most acutely toxic chemicals to aquatic organisms ever deliberately introduced to water"* (Maguire 1987). They alter fat storage in the freshwater crustacean *Daphnia magna*, impact feeding at EC_{50} = 3 µg/L, and decrease body length and offspring size at solution concentrations near 1 µg/L (Jordão et al. 2016). Dialkytins exhibit lower toxicity than trialkytins, but they can still be highly toxic to aquatic organisms. Tributyltin chloride $(C_4H_9)_3SnCl$, for example, exhibits a 24-hour LC_{50} = 0.95 µg/L to *D. magna*, while dibutyltin diacetate $(C_4H_9)_2Sn(CH_3COO)_2$, with a corresponding LC_{50} = 0.17 mg/L, is much less toxic (Kungolos et al. 2004). In addition, dibutyltin and dioctyltin can induce thymus atrophy and effects on the immune system (Arakawa 1998; Arakawa et al. 1980; Seinen and Willems 1976). Research evaluating the toxicity of organotin compounds to algae species *Ankistrodemus falcatus* indicates trialkyltin compounds are the most toxic, followed by dialkyl, and monoalkyltin species (Wong et al. 1982). This study is consistent with the general trend in organotin toxicity based on alkyl substitution where $RSnX_3$ (monoalkyltin) < R_2SnX_2 (dialkyltin) < R_4Sn (tetraalkyltin) ≪ R_3SnX

(trialkyltin) (Kerk et al. 1954; Van der Kerk and Luijten 1956; Winship 1987). In addition, for the same degree of alkyl substitution, the longer chain carbon groups with higher solubility in octanol were more toxic to the algae, as demonstrated by minimum inhibition concentrations for *Ankistrodesmus falcatus* primary productivity: Bu_3Sn: 0.02 mg/L; Bu_2Sn: 6.8 mg/L; BuSn: 25 mg/L (Wong et al. 1982). These compounds can not only elicit adverse impacts to lower level freshwater species, some of them are also considered as endocrine-disrupting chemicals, which can affect the health of higher level organisms (Berto-Júnior et al. 2018). For instance, tributyltin often used as an antifouling agent applied on a ship's hull can constantly release into the water and become adsorbed by marine species. Researchers previously found that it can bioaccumulate and biomagnify in the ecosystem.

The severe toxicity of trialkyl- and dialkyl-tin compounds inevitably raises environmental concerns about new applications and eventual disposal of new alkyltin systems. While simple, molecular monoalkyltin compounds are much less toxic than their di- and tri-alkyltin analogues (Stoner et al. 1955), no environmental studies of monoalkyltin compounds in condensed-cluster and thin-film forms have been reported. Grenville and co-workers have recently introduced new monoalkyltin-based oxo-hydroxo clusters and films to support the introduction of EUV lithography in the semiconductor industry (Grenville et al. 2015). This work is based on the high EUV absorption cross section of tin and the associated radiolytic efficiency of Sn-C bond scission (Cardineau et al. 2014), which together enable transformational patterning performance for production of features at single-digit-nm resolution. These clusters and films are now being distributed to all major semiconductor manufacturers. The Registration, Evaluation, Authorization and Restriction of Chemicals (REACH) regulation dictates chemicals and nanoparticles sold in the European market in

volumes greater than one ton per year must be characterized for potential impact on aquatic ecosystems (European Commission 2006). In addition, many researches have indicated that a chemical species in nanoscale could exhibit different bioavailability and toxicity than their bulk forms, such as ions and molecules (Böhme et al. 2017; Bollyn et al. 2018; Denluck et al. 2018; Jiang et al. 2017); therefore, it is particularly important to understand the potential environmental implications before scaling up for application. The aim of this study was to determine whether monoakyl tin clusters are environmentally friendly materials for large-scale use in the semiconductor industry. Thus, we performed a toxicological assessment using algae and crustaceans on synthesized *BuSn* nano-clusters and leachate collected from the thin films under varying environmental conditions.

MATERIALS AND METHODS

Synthesis of BuSn

BuSn was prepared based on slightly modified literature procedures (Eychenne-Baron et al. 1998). BuSnOOH (20.0 g) and p-toluene sulfonic acid (TsOH) monohydrate (5.77 g) were suspended in toluene and refluxed with a Dean-Stark trap for 48 h. After centrifugation to remove solids, the supernatant was removed under reduced pressure to yield solid $[(BuSn)_{12}O_{14}(OH)_6][OTs]_2$, which was washed with acetonitrile and allowed to dry in an open container (45% yield). A 20 wt% suspension of $[(BuSn)_{12}O_{14}(OH)_6][OTs]_2$ was created by mixing 2.00 g of $[(BuSn)_{12}O_{14}(OH)_6][OTs]_2$ with 8.00 g isopropanol. Separately a 65-wt% solution of tetramethylammonium hydroxide (TMAH) was prepared by mixing 1.69 g TMAH solution (1 M aqueous concentration) with isopropanol to get a total mass of 2.3 g. With vigorous stirring, the TMAH solution was added all at once to the suspension of

$[(BuSn)_{12}O_{14}(OH)_6][OTs]_2$. After stirring for 30 minutes, the suspension was more homogenous but still remained slightly turbid, and without filtering was placed in a vial in the freezer (-20°C). After 2-3 days, needle shaped crystals of $[(BuSn)_{12}O_{14}(OH)_6][OH]_2$ had formed and were isolated and washed with acetonitrile (28% yield). We confirmed purity using ^{119}Sn and ^{13}C NMR (data not shown). The structure is shown in Figure 1.

Film Preparation

N-type Si (100) wafers with native oxide and SiO_2/Si (100) wafers with 100 nm of thermally grown SiO_2 were obtained from Sumco Oregon Corporation and Silicon Valley Microelectronics, Inc., respectively. Prior to thin film deposition, all substrates were cleaned thoroughly in a bath of deionized water by sonication. Following this rinse, the surfaces were treated with low-energy O_2 plasma, creating a clean, hydrophilic surface. Solutions of *BuSn* were created through dissolution of 80 mg/mL of the solid in 2-heptanone to yield a saturated solution. Following dissolution, the solution was then filtered and 1 mL of the supernatant dried and calcined at 1000°C to determine concentration with respect to tin (as tin (IV) oxide). The concentration of the saturated solution was thus determined to be 0.04M. Films were spin-coated at 3000 rpm for 30s on the Si(100) wafers using 0.04M *BuSn* dissolved in 2-heptanone. Films were then soft-baked for three minutes at 70°C to remove residual solvent.

Film Characterization

Film Thickness. Ellipsometry data was collected on a JA Woollam MX-2000 ellipsometer. Data were collected over the interval from 400-1000 nm and modeled using the Cauchy equation. Thickness and refractive index (n) were extracted and

mean square error (MSE) was used to determine goodness of fit. Film thickness was confirmed by step-height measurement with atomic force microscopy (AFM, Park Systems NX-10 instrument). AFM measurements were done in non-contact mode with a PPP-NCHR tip (Nanosensors, tip radius < 10 nm). Samples were prepared for step-height measurements by dipping one edge of the as-deposited films into 2-heptanone for 30s to partially rinse away the film and create a step-edge between the film and substrate. Following rinsing, the films were dried with nitrogen, and again soft-baked at 70°C to evaporate any residual solvent.

Film Surface Morphology. Images were collected using a Veeco di-Innova AFM in tapping mode. The collection parameters for each experiment were set to 32 x 32 pixel resolution, using 5 µm/s scan rate over a 5 x 5 µm scan size. The aspect ratio for the images is 1.00 and the amplitude set point was 1716.62 mV. Each image was processed using a 3rd order plane fit and flattening filters with the Bruker Nanoscope Analysis 1.5 software.

Time-of-Flight Secondary Ion Mass Spectrometry (TOF-SIMS). TOF-SIMS was collected using an ION-TOF Model IV Time-of-Flight Secondary Ion Mass Spectrometer. Cs ions were used as the sputter source, and the instrument was equipped with a Bi nanoprobe for better data resolution. 1x1 inch films of the precursors were mounted on an aluminum sample holder using carbon tape before sputtering with a Cs ion source. Owing to the nature of the experiment and the need for increased thickness due to sputter depth profiling of the thin film samples, the concentrations of the precursor solutions were increased.

X-ray photoelectron spectroscopy (XPS). XPS data were collected using a PHI 5600 spectrometer with a base pressure of $<1x10^{-9}$ mbar and non-monochromatized

Mg Kα X-rays (1253.6 eV). The electron analyzer was set to a pass energy of 29.35 eV, with a 45° emission angle and 54.7° source-analyzer angle. Energy scale linearity was calibrated to Au $4f_{7/2}$ at 84.0 eV and Cu $2p_{3/2}$ at 932.7 eV. All spectra were charge corrected to the C 1s aliphatic carbon peak at 284.8 eV (Moulder et al. 1992). XPS spectra were fit with CasaXPS using a linear background and Gaussian-Lorentzian peak shape. Atomic concentrations were calculated using instrument specific published sensitivity factors corrected for the transmission function of the analyzer (Moulder et al. 1992).

Leachate Collection

Ultrapure water with 10 mM of HEPES buffer was prepared and the pH was adjusted with 0.5 M NaOH to 5.6 and 7, respectively. No solvents were used to simulate what would occur in a landfill. Thin films were each placed in 50 ml each of four incubation scenarios: Temp = 20°C, pH = 7; Temp = 20°C, pH = 5.6; Temp = 37°C, pH = 7; and Temp = 37°C, pH = 5.6). Triplicate incubations were prepared for 14 and 90-day toxicity evaluations and tin leaching kinetics. To evaluate tin leaching kinetics, a 5 mL sample was collected from each beaker at days 1, 7, 14, 60 and 90. Collected leachate samples were digested with 69% trace-metal grade nitric acid (Sigma Aldrich, St. Louis, MO) at 200°C in teflon tubes. Once the acid had completely evaporated, the acidification and evaporation process was repeated two more times. Trace-metal grade nitric acid (0.15 ml) was added to each teflon tube while the tube was still hot, followed by 4.85 ml acidified indium solution (3% nitric acid and 1 μg L^{-1} internal indium standard) bringing the final sample volume to 5 ml. Samples were analyzed for tin concentration by Inductively coupled plasma mass spectrometry (ICP-MS) (Thermo Fisher Scientific, Waltham, MA) (Wu et al. 2017).

Tin and indium ICP standards were purchased from Ricca Chemical Company (Arlington, TX). All samples were measured in triplicate.

Toxicity Testing

BuSn nano-cluster stock solution was prepared at 500 mg/L in ultrapure water (18.2 MΩ·cm at 25 °C Milli-Q Water) and ultrasonicated for 1, 6, 16, and 31 minutes at maximum intensity using a VCX 750 Vibra-Cell ultrasonicator (Sonics & Materials Inc., Newtown, CT) equipped with a cup-horn style probe and recirculating water bath to maintain temperature. The smallest hydrodynamic diameter (HDD) and polydispersity index (PDI) values were determined at after 1 minute of sonication (Figure S1). Freshly prepared stock solutions were similarly ultrasonicated for 1 minute prior to exposing organisms. TAP media was used for the algal exposure media (Gorman and Levine 1965), and *D. magna* exposure media was adapted from the EPA hard water recipe consisting of sodium bicarbonate (192 mg L^{-1}), calcium sulfate dihydrate (120 mg L^{-1}), magnesium sulfate (120 mg L^{-1}) and potassium chloride (6 mg L^{-1}). *Chlamydomonas reinhardtii* (*C. reinhardtii*) was selected as the model organism. In algae exposures, the initial algal population density was fixed at 10^4 cells/mL with a final volume of 5 mL in a 15 mL glass vial, and the exposure concentrations of *BuSn* nano-cluster were 0, 15.6, 31.3, 62.5, 125, 250 mg/L. Stock and working solutions were vortexed prior to exposure to ensure the particles were well-suspended. Algal exposure vials were placed on shaker table at 120 rpm during the experimental period. All organisms and experiments were maintained and conducted at 20.5 ± 0.5 °C with a 16:8-h light:dark photoperiod under 1690 ± 246 lux light intensity provided by full-spectrum fluorescent grow lights. For toxicity evaluation of collected leachate, the pH was first adjusted back to 7.0 with 0.5M

NaOH solution. Concentrated (100x) algae (TAP media) and *D. magna* exposure media (EPA hard water) were diluted using each collected leachate to provide essential nutrients during toxicity testing. The toxicity of each collected leachate was evaluated by exposing algae for 72 hours and evaluating growth and exposing *D. magna* for 48 hours to monitor mortality and immobilization.

Algal viability was measured using SYTOX™ Green Dead Cell Stain (Life Technologies, Grand Island, NY) in conjunction with flow cytometry at 3, 20, 28, 48 and 72 hours of growth. Algal growth rates were modeled using a first order exponential growth model. For *D. magna* acute toxicity testing, five neonates (<24 hours) with 10 mL daphnia culture media in a 50 mL plastic beaker were exposed to $(BuSn)_{12}(OH)_6$ crystals at concentrations of 50, 100, 125, 150, 175, 200, 225, 250 mg L^{-1}. Mortality and immobilization were recorded at 24 and 48 hours. Each treatment was conducted in triplicate for a total of 15 neonates at each concentration.

Data Analysis

SigmaPlot version 13.0 (Systat Software, San Jose, CA, USA) was used to perform all statistical analyses. Differences in toxicity were compared using analysis of variance (ANOVA) with Dunnett's post-hoc analysis. All differences were considered statistically significant at $p \leq 0.05$. Tin leaching over the 90 day test period were calculated by fitting a first order kinetic model:

$$[Sn] = [Sn]_{max}\,[1 - e^{-kt}] \qquad \text{(Equation 1)}$$

Where $[Sn]_{max}$ is the predicted maximum amount of tin released from the thin films, k is the leaching rate of tin (day^{-1}) and t represents the time (day).

RESULTS AND DISCUSSION

Film Characterization

We used ellipsometry and AFM to study film thickness and surface morphology, respectively. Figure 2 shows the 2D and 3D images of the cluster spun into film. The Root Mean Square (RMS) roughness (R_q) for this film was 6.09 nm. Defects are seen in the film in AFM and confirmed with XPS. Film non-uniformity was clearly observed using AFM, where a distribution of islands up to 40 nm thick were observed. The cluster is largely non-polar and spinning a non-polar precursor onto a hydrophilic surface may results in crystallization/aggregation as the cluster is more attracted toward itself than to the surface. Studies are ongoing to optimize the films; however, this film was chosen to study the toxicity because we expected the higher surface area would lead to a larger leach rate and thus anticipated greater toxicity than flatter films.

TOF-SIMS and XPS were used to study composition. Figure 3 shows the TOF-SIMS survey scans of the films, which confirm XPS data (Figure S2). The films contain primarily Sn, C, and O. XPS results indicate that the atomic percents for Sn, C, and O are 17%, 56%, and 28%, which is within 2-3% of the expected composition (Table S1). Trace amounts of Cl are seen in the film with TOF-SIMS that are undetectable with XPS , likely as a residual following initial synthesis from n-butyltin oxide hydroxide hydrate. Also seen only in TOF-SIMS data is S in trace amounts as a residual species, introduced through use of tosylic acid as a counterion in the initial synthesis of the cluster. TOF-SIMS and XPS data also show the predominant oxidation state of Sn. Sn (as Sn^{4+}) is the majority of tin present as Sn bonded to O in the football cluster.

Toxicity of BuSn Nano-clusters

The ecotoxicity of the organotin clusters suspensions was investigated by exposing freshwater algae and plankton to them. In accordance with OECD (201, 211) methods (OECD 2011; 2012), we assessed the impact of pure *BuSn* clusters on 72-hour growth inhibition to *Chlamydomonas reinhardtii* and 48-hour immobilization and mortality to neonate *D. magna* at exposure concentrations up to 250 mg/L. The organotin clusters had no impact on algal growth rates up to 250 mg/L (Figure 4), whereas Figure 5 shows immobilization and mortality significantly increased for *D. magna* at concentrations ≥100 mg/L. Although *Daphnia* mortality was significantly increased at 100 mg/L, the higher concentrations did not result in significant mortality or immobilization. These findings suggest that at the higher exposure concentrations, the nanoparticles are likely agglomerating in the *Daphnia* media and settling out of the water column during the exposure. The increased toxic response of *D. magna* relative to the algae, likely reflects the high sensitivity of *Daphnia* to particulate toxins due to their filter feeding behavior. The suspended *BuSn* nanoparticles exhibit an EC_{50} = 45.9 ± 24.4 mg L^{-1} to *D. magna.* Therefore, based on the Environmental Protection Agency's Ecotoxicity Categories for Terrestrial and Aquatic Organisms (National Research Council 2014), *BuSn* cluster toxicity is considered *slightly toxic* to *D. magna* but *practically non-toxic* category for *C. reinhardtii*.

The large variance in the estimated EC_{50} values likely arises from the hydrophobicity of *BuSn* clusters and their tendency to agglomerate at high concentrations, which leads to inhomogeneous bioavailability to target organisms (Hotze et al. 2010). The hydrodynamic diameter (HDD), a measure of the size of the agglomerated clusters, reached a minimum after 1 minute of ultra-sonication, then

significantly increased by 2-fold after 30 minutes of sonication (Figure S1). BuSn clusters are largely agglomerated due to the lack of surface stabilizers in the suspended media. Meanwhile, it is likely that the charge state, +2, of the cluster and the charge balancing counterion OH^- produce significant surface charges and intercluster interactions, which leads to agglomerate formation (Baalousha et al. 2013). The agglomerates grow with sonication time, this phenomenon was also observed previously by Pradhan et al., where they suggest the strong van der Waals forces of the metal NPs resulted in significant NP agglomeration and sedimentation (Pradhan et al. 2016). The increasing in agglomeration size could also be caused by the high Brownian motion produces particle-cluster collisions and new interparticle electrostatic interactions.

Leachate Characterization

In manufacturing, the semiconductor industry is likely to etch or thermally oxidize the *BuSn* coatings to benign SnO_2. Nevertheless, *BuSn*-coated wafers end-of-life leachate contamination was evaluated via simulated and controlled laboratory conditions that mimic landfill conditions. A well-designed landfill should have a long residence time for the leachate (LaGrega et al. 2010), which can range from weeks to years depending on site location and seasonal hydrological dynamics (Mangimbulude et al. 2009). In addition, leachate pH may vary dramatically both spatially and temporally (Christensen et al. 2001). Commonly, initial leachate exhibits a low pH from high concentrations of degradable organic compounds and heavy metals; it can be as low as pH 5 in some extreme situations (Renou et al. 2008). Over time, the landfill enters the methanogenic phase and produces CH_4, which increases pH. To simulate these landfill conditions and investigate the potential end-of-life impacts of

our coated wafers, we studied short-term (14 day) and long-term (90 day) leaching scenarios in water at pH = 5.6 and 7.0 and T = 20 and 37°C. These studies evaluate the stability of the coatings to varying environmental conditions and the differences in toxicity of solid *BuSn* and its leachate.

The leached tin concentrations were quantified at 1, 7, 14, 30, 60, and 90 days. Significantly, more tin leached from the coated wafers compared with uncoated control wafers in all four incubation scenarios (Figure S3 & S4). A first-order kinetic model describes the rate of tin leaching (Figure 6a). Equation 1 (see Methods 2.5) describes maximum leaching capacity and tin leaching rates in each incubation scenario (Figure 6a). Tin leaching capacity is highest in the 37°C, pH = 7 incubation scenario at 0.74 µg Sn/cm^2, and lowest at 37°C and pH = 5.6 at 0.24 µg Sn/cm^2 (Figure 6b). Tin releases rapidly in all four incubation scenarios from day 0 to day 14; however, the modeled rates suggest pH is responsible for accelerating tin leaching (Figure 6c), with lower pH at 5.6 had higher tin leaching rates than pH at 7.0. After 14 days, tin leaching reaches a plateau. The total film mass applied to the 1-cm^2 wafer corresponds to 23.74 µg of tin, which suggests only 1.1 to 3.4% of the deposited tin leaches from the wafers after 90 days. The variation in the amount of tin leached depends on the incubation scenario. On average, we estimate 6.2 m^2 of coated wafers need to be soaked in 1 L of water to reach the EC_{50} for *D. magna*. Thus, coated wafers will only impact aquatic species adversely, if they are disposed in large quantities, then incubated in water-rich environments. Importantly, the tin leaching kinetics show the released tin concentration reaches a plateau within the first month, which suggests long leaching times minimally affect total tin release.

Wafer Leachate Toxicity

Wafer leachate toxicity was evaluated by both algae (*C. reinhardtii*) and crustaceans (*D. magna*). Figure S5 shows no significant difference in algal growth based on timeframe, pH, or temperature. Figure 7 shows *D. magna* mortality and immobilization after exposure to each collected leachate. 14-day leachate exposure produces no significant mortality and immobilization (Figure 7a). Both control and tin coated wafers leached at 37°C, however, caused significantly higher immobilization (Figure 7b). The toxicity observed from both control and coated wafer leachates collected at 37 °C suggests an unknown chemical species leaches from the silicon wafers and causes the observed immobilization. Further analysis is required to identify this toxic agent. No significant difference was observed in toxicity between control and *BuSn*-coated wafer leachates. We expect a low toxicity, since the released tin concentrations are substantially lower than those concentrations that elicited responses in the exposed aquatic organisms.

Environmental degradation may further reduce potential adverse impacts of these tin wafers to aquatic organisms. For example, reports describe how photolysis and biological degradation affect the persistence of trialkyltin compounds in aquatic ecosystems and sediments. The reported photolytic half-life ($T_{1/2}$) of butyltin compounds in water under sunlight is about 89 days (Luijten 1972), and may be as short as 18 days (Slesinger and Dressler 1978) or shorter via a combination of sunlight and microbial degradation (Maguire et al. 1983; Seligman et al. 1989).

Conclusion

This is a pilot study focused on evaluating the newly developed mono- tin ecotoxicity on algae and crustaceans. The results of our ecotoxicology and leachate

studies provide robust evidence that *C. reinhardtii* and *D. magna* exhibit low toxicity to suspensions of *BuSn* and the leachate from *BuSn*-coated wafers. Although the ecotoxicity of higher level organisms was not evaluated in current study, it is essential and necessary to investigate further the safety of this new class of inorganic photoresist. Future work will also focus on case studies that address ecotoxicity of the materials across the many steps of lithography applied in semiconductor manufacturing.

Supplemental Data—The Supplemental Data are available on the Wiley Online Library at DOI: 10.1002/etc.xxxx.

Acknowledgment— Cluster and thin film synthesis and characterization were supported by the Center for Sustainable Materials Chemistry under awards: NSF CHE -1102637 and CHE-1060982. Ecotoxicity studies were supported by NSF: 1438165, and the Oregon Nanoscience and Microtechnologies Institute.

Data accessibility— Please contact the corresponding author for any meta data or calculations not already provided.

References

Arakawa Y. 1998. Recent studies on the mode of biological action of di-and trialkyltin compounds. Chemistry of tin. Springer. p. 388-428.

Arakawa Y, Yamazaki N, Yu T, Nagahashi M. 1980. Effects of organotin compounds on the immune functions: Atrophy of thymus by di-n-butyltin dichloride. Journal of toxicological sciences. 5(3):258.

Baalousha M, Nur Y, Römer I, Tejamaya M, Lead J. 2013. Effect of monovalent and divalent cations, anions and fulvic acid on aggregation of citrate-coated silver nanoparticles. Science of the Total Environment. 454:119-131.

Berto-Júnior C, de Carvalho DP, Soares P, Miranda-Alves L. 2018. Tributyltin and zebrafish: Swimming in dangerous water. Frontiers in endocrinology. 9:152.

Böhme S, Baccaro M, Schmidt M, Potthoff A, Stärk H-J, Reemtsma T, Kühnel D. 2017. Metal uptake and distribution in the zebrafish (danio rerio) embryo:

Differences between nanoparticles and metal ions. Environmental Science: Nano. 4(5):1005-1015.

Bollyn J, Willaert B, Kerré B, Moens C, Arijs K, Mertens J, Leverett D, Oorts K, Smolders E. 2018. Transformation-dissolution reactions partially explain adverse effects of metallic silver nanoparticles to soil nitrification in different soils. Environmental toxicology and chemistry. 37(8):2123-2131.

Cardineau B, Del Re R, Marnell M, Al-Mashat H, Vockenhuber M, Ekinci Y, Sarma C, Freedman DA, Brainard RL. 2014. Photolithographic properties of tin-oxo clusters using extreme ultraviolet light (13.5 nm). Microelectronic Engineering. 127:44-50.

Christensen TH, Kjeldsen P, Bjerg PL, Jensen DL, Christensen JB, Baun A, Albrechtsen H-J, Heron G. 2001. Biogeochemistry of landfill leachate plumes. Applied geochemistry. 16(7):659-718.

National Research Council. 2014. A framework to guide selection of chemical alternatives. National Academies Press.

Davies AG, Smith PJ. 1980. Recent advances in organotin chemistry. Advances in inorganic chemistry and radiochemistry. 23:1-77.

Denluck L, Wu F, Crandon LE, Harper BJ, Harper SL. 2018. Reactive oxygen species generation is likely a driver of copper based nanomaterial toxicity. Environmental Science: Nano. 5(6):1473-1481.

Eychenne-Baron C, Ribot F, Sanchez C. 1998. New synthesis of the nanobuilding block $(busn)_{12}o_{14}(oh)_6^{2+}$ and exchange properties of $(busn)_{12}o_{14}(oh)_6(o_3sc_6h_4ch_3)_2$. Journal of organometallic chemistry. 567(1):137-142.

Gorman DS, Levine R. 1965. Cytochrome f and plastocyanin: Their sequence in the photosynthetic electron transport chain of chlamydomonas reinhardi. Proceedings of the National Academy of Sciences. 54(6):1665-1669.

Grenville A, Anderson JT, Clark BL, De Schepper P, Edson J, Greer M, Jiang K, Kocsis M, Meyer ST, Stower JW. 2015. Integrated fab process for metal oxide euv photoresist. SPIE Advanced Lithography: International Society for Optics and Photonics.

Horiguchi T. 2017. Contamination by organotins and its population-level effects involved by imposex in prosobranch gastropods. Biological effects by organotins. Springer. p. 73-99.

Hotze EM, Phenrat T, Lowry GV. 2010. Nanoparticle aggregation: Challenges to understanding transport and reactivity in the environment. Journal of environmental quality. 39(6):1909-1924.

Jiang C, Castellon BT, Matson CW, Aiken GR, Hsu-Kim H. 2017. Relative contributions of copper oxide nanoparticles and dissolved copper to cu uptake

kinetics of gulf killifish (fundulus grandis) embryos. Environmental science & technology. 51(3):1395-1404.

Jordão R, Garreta E, Campos B, Lemos MF, Soares AM, Tauler R, Barata C. 2016. Compounds altering fat storage in daphnia magna. Science of the Total Environment. 545:127-136.

Kerk V, Der G, Luijten J. 1954. Investigations on organo-tin compounds. Iii. The biocidal properties of organo-tin compounds. Journal of Applied Chemistry. 4(6):314-319.

Kungolos A, Hadjispyrou S, Petala M, Tsiridis V, Samaras P, Sakellaropoulos G. 2004. Toxic properties of metals and organotin compounds and their interactions on daphnia magna and vibrio fischeri. Water, Air and Soil Pollution: Focus. 4(4-5):101-110.

LaGrega MD, Buckingham PL, Evans JC. 2010. Hazardous waste management. Waveland Press.

Luijten J. 1972. Applications and biological effects of organotin compounds. Organotin compounds. 3:931-974.

Maguire RJ. 1987. Environmental aspects of tributyltin. Applied Organometallic Chemistry. 1(6):475-498.

Maguire RJ, Carey JH, Hale EJ. 1983. Degradation of the tri-n-butyltin species in water. Journal of Agricultural and Food Chemistry. 31(5):1060-1065.

Mangimbulude JC, van Breukelen BM, Krave AS, van Straalen NM, Röling WF. 2009. Seasonal dynamics in leachate hydrochemistry and natural attenuation in surface run-off water from a tropical landfill. Waste Management. 29(2):829-838.

Moulder JF, Stickle WF, Sobol PE, Bomben KD. 1992. Handbook of x-ray photoelectron spectroscopy. 1992. Perkin Elmer Corporation p61.

OECD. 2011. Test no. 201: Freshwater alga and cyanobacteria, growth inhibition test. OECD Guidelines for the Testing of Chemicals, Section 2. Paris: OECD Publishing. p. 25.

OECD. 2012. Test no. 211: *Daphnia magna* reproduction test. OECD Guidelines for the Testing of Chemicals, Section 2. Paris: OECD Publishing.

European Commission. 2006. Regulation (ec) no. 1907/2006 of the european parliament and of the council of 18 december 2006 concerning the registration, evaluation, authorisation and restriction of chemicals (reach), establishing a european chemicals agency, amending directive 1999/45/ec and repealing council regulation (eec) no. 793/93 and commission regulation (ec) no. 1488/94 as well as council directive 76/769/eec and commission directives 91/155/eec, 93/67/eec, 93/105/ec and 2000/21/ec. Official Journal of the European Union. 396.

Pradhan S, Hedberg J, Blomberg E, Wold S, Wallinder IO. 2016. Effect of sonication on particle dispersion, administered dose and metal release of non-functionalized, non-inert metal nanoparticles. Journal of nanoparticle research. 18(9):285.

Renou S, Givaudan J, Poulain S, Dirassouyan F, Moulin P. 2008. Landfill leachate treatment: Review and opportunity. Journal of hazardous materials. 150(3):468-493.

Seinen W, Willems MI. 1976. Toxicity of organotin compounds. I. Atrophy of thymus and thymus-dependent lymphoid tissue in rats fed di-n-octyltindichloride. Toxicology and applied pharmacology. 35(1):63-75.

Seligman PF, Grovhoug JG, Valkirs AO, Stang PM, Fransham R, Stallard MO, Davidson B, Lee RF. 1989. Distribution and fate of tributyltin in the united states marine environment. Applied Organometallic Chemistry. 3(1):31-47.

Slesinger AE, Dressler I. 1978. The environmental chemistry of three organotin chemicals. Report of the Organotin Workshop Good, M(Ed) University of New Orleans, New Orleans, LA.

Stoner H, Barnes J, Duff JI. 1955. Studies on the toxicity of alkyl tin compounds. British journal of pharmacology and chemotherapy. 10(1):16-25.

Van der Kerk G, Luijten JGA. 1956. Investigations on organo-tin compounds. V the preparation and antifungal properties of unsymmetrical tri-n-alkyltin acetates. Journal of Applied Chemistry. 6(2):56-60.

Winship K. 1987. Toxicity of tin and its compounds. Adverse drug reactions and acute poisoning reviews. 7(1):19-38.

Wong P, Chau Y, Kramar O, Bengert G. 1982. Structure-toxicity relationship of tin compounds on algae. Canadian Journal of Fisheries and Aquatic Sciences. 39(3):483-488.

Wu F, Harper BJ, Harper SL. 2017. Differential dissolution and toxicity of surface functionalized silver nanoparticles in small-scale microcosms: Impacts of community complexity. Environmental Science: Nano. 4(2):359-372.

FIGURES

Figure 1. Chemical Structure of BuSn.

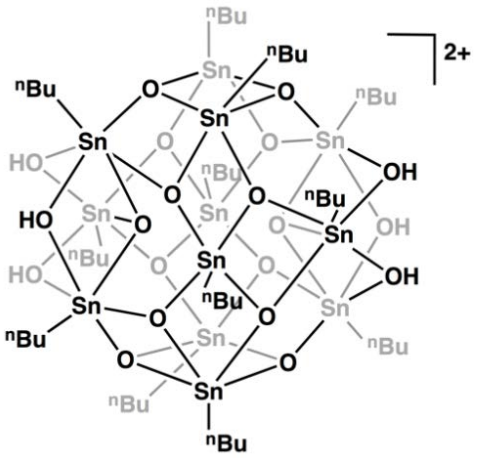

Figure 2. AFM images of the film from $[(BuSn)_{12}O_{14}(OH)_6][OH]_2$ compound in 2-heptanone. [Sn] = 0.08M.

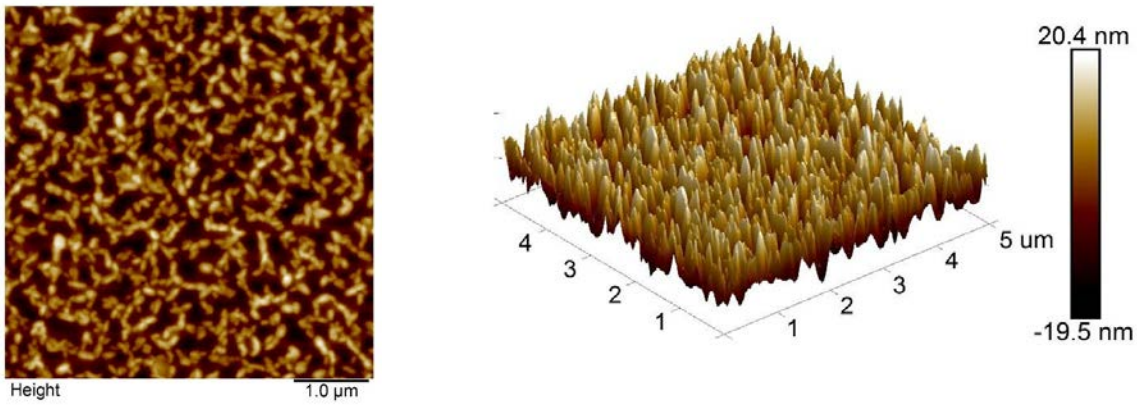

Figure 3. TOF-SIMS spectra of a film prepared with $[(BuSn)_{12}O_{14}(OH)_6][OH]_2$.

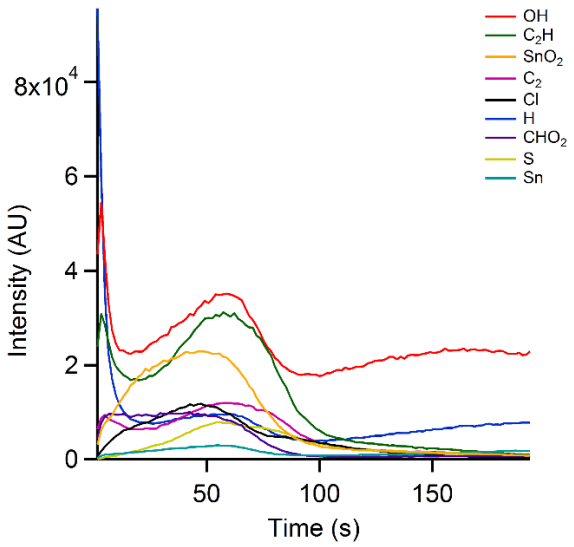

Figure 4. Toxicity of BuSn nano-clusters measured as C. reinhardtii growth rates.

Error bars represent standard error of three sample replicates.

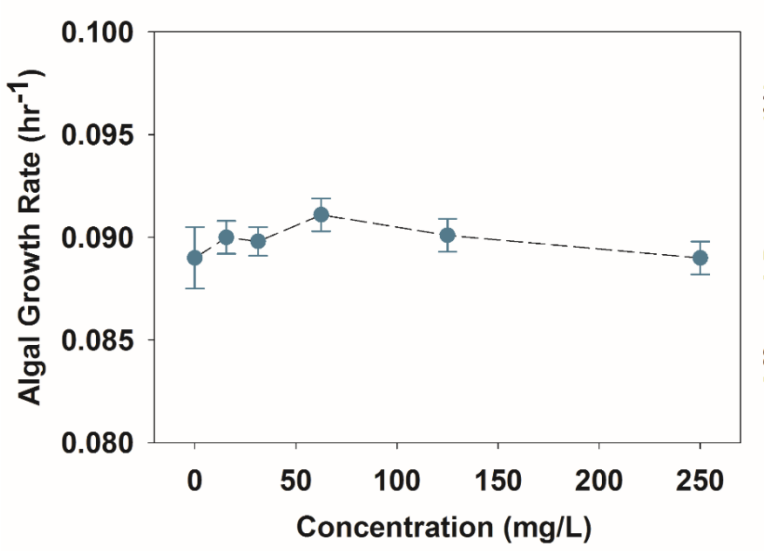

Figure 5. Toxicity of BuSn nano-clusters measured as D. magna immobilization and mortality. Error bars represent standard error of three sample replicates. Asterisk (*)indicates significantly different immobilization and octothorp (#) shows significantly different mortality compared to control.

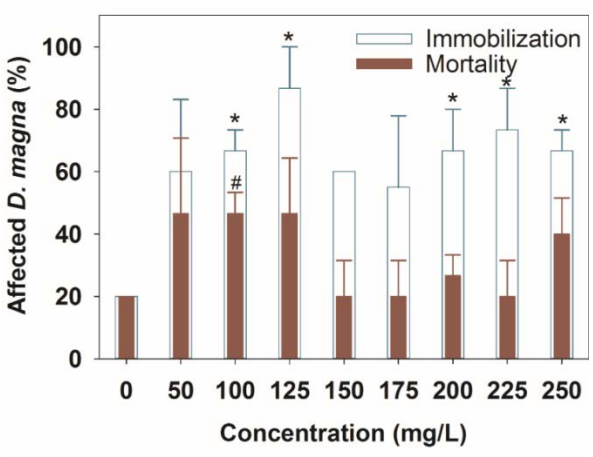

Figure 6. Tin release kinetics of tin coated wafers (a), modeled leaching capacity over 90 days (b), and the leaching rate of tin from wafers (c) under four different environmental scenarios. Error bars in panel a represent standard error of measured tin leaching concentration of triplicate measurements. Error bars in panel b and c represent standard error of modeled values. Asterisk (*) and octothorp (#) indicate significant difference among varying incubation scenarios.

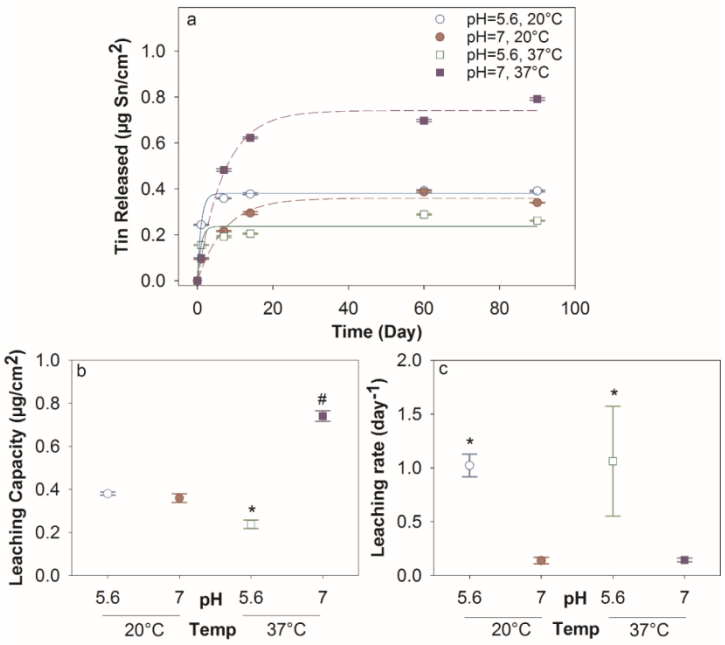

Figure 7. D. magna 48-hour immobilization and mortality after exposure to wafer leachate after 14 (a) and 90 (b) days of leaching. (CW: Control wafer; TW: Tin-coated wafer). Asterisks (*) indicate significant difference in D. magna immobilization between 14 and 90 days with the same type wafer leachate exposure. Error bars represent standard error of three replicates.